ISSN 1674-1056
http://cpb.iphy.ac.cn
http://iopscience.iop.org/cpb
中国物理 B
Chinese Physics
中国物理 Chinese Physics B

Molecule opacities of $X^2\Sigma^+$, $A^2\Pi$, and $B^2\Sigma^+$ states of CS^+

Xiao-He Lin(林晓贺), Gui-Ying Liang(梁桂颖), Jian-Guo Wang(王建国), Yi-Geng Peng(彭裔耕), Bin Shao(邵彬), Rui Li(李瑞), Yong Wu(吴勇)

Citation: Chin. Phys. B . 2019, 28(5): 053101. **doi:** 10.1088/1674-1056/28/5/053101
Journal homepage: http://cpb.iphy.ac.cn; http://iopscience.iop.org/cpb

What follows is a list of articles you may be interested in

Explicitly correlated configuration interaction investigation on low-lying states of SiO^+ and SiO

Rui Li(李瑞), Gui-Ying Liang(梁桂颖), Xiao-He Lin(林晓贺), Yu-Hao Zhu(朱宇豪), Shu-Tao Zhao(赵书涛), Yong Wu(吴勇)
Chin. Phys. B . 2019, 28(4): 043102. **doi:** 10.1088/1674-1056/28/4/043102

Diffusion Monte Carlo calculations on LaB molecule

Nagat Elkahwagy, Atif Ismail, S M A Maize, K R Mahmoud
Chin. Phys. B . 2018, 27(9): 093102. **doi:** 10.1088/1674-1056/27/9/093102

Theoretical study of spin-forbidden cooling transitions of indium hydride using *ab initio* methods

Yun-Guang Zhang(张云光), Hua Zhang(张华), Ge Dou(窦戈)
Chin. Phys. B . 2017, 26(9): 093101. **doi:** 10.1088/1674-1056/26/9/093101

Potential energy curves, transition dipole moments, and radiative lifetimes of KBe molecule

Ming-Jie Wan(万明杰), Cheng-Guo Jin(金成国), You Yu(虞游), Duo-Hui Huang(黄多辉), Ju-Xiang Shao(邵菊香)
Chin. Phys. B . 2017, 26(3): 033101. **doi:** 10.1088/1674-1056/26/3/033101

Low-lying electronic states of CuN calculated by MRCI method

Shu-Dong Zhang(张树东), Chao Liu(刘超)
Chin. Phys. B . 2016, 25(10): 103103. **doi:** 10.1088/1674-1056/25/10/103103

Molecule opacities of $X^2\Sigma^+$, $A^2\Pi$, and $B^2\Sigma^+$ states of CS^+*

Xiao-He Lin(林晓贺)[1,2,†], Gui-Ying Liang(梁桂颖)[2,†], Jian-Guo Wang(王建国)[2], Yi-Geng Peng(彭裔耕)[2], Bin Shao(邵彬)[1], Rui Li(李瑞)[2,3,‡], and Yong Wu(吴勇)[2,4,§]

[1] *School of Physics, Beijing Institute of Technology, Beijing* 100081, *China*
[2] *Institute of Applied Physics and Computational Mathematics, Beijing* 100088, *China*
[3] *Department of Physics, College of Science, Qiqihar University, Qiqihar* 161006, *China*
[4] *HEDPS, Center for Applied Physics and Technology, Peking University, Beijing* 100084, *China*

(Received 29 January 2019; revised manuscript received 28 February 2019; published online 4 April 2019)

Carbon sulfide cation (CS^+) plays a dominant role in some astrophysical atmosphere environments. In this work, the rovibrational transition lines are computed for the lowest three electronic states, in which the internally contracted multireference configuration interaction approach (MRCI) with Davison size-extensivity correction (+Q) is employed to calculate the potential curves and dipole moments, and then the vibrational energies and spectroscopic constants are extracted. The Frank–Condon factors are calculated for the bands of $X^2\Sigma^+$–$A^2\Pi$ and $X^2\Sigma^+$–$B^2\Sigma^+$ systems, and the band of $X^2\Sigma^+$–$A^2\Pi$ is in good agreement with the available experimental results. Transition dipole moments and the radiative lifetimes of the low-lying three states are evaluated. The opacities of the CS^+ molecule are computed at different temperatures under the pressure of 100 atms. It is found that as temperature increases, the band systems associated with different transitions for the three states become dim because of the increased population on the vibrational states and excited electronic states at high temperature.

Keywords: CS^+, dipole moment, transition dipole moment, opacity

PACS: 31.50.Df, 31.15.ag, 31.15.aj **DOI:** 10.1088/1674-1056/28/5/053101

1. Introduction

Carbon sulfide cation (CS^+) has received considerable attention owing to its dominant role in spectroscopy and astrophysics. In astrophysics, several sulfur compounds[1–6] (CS, CS^+, HCS^+, C_2S, C_3S, and C_5S) have been observed in interstellar molecular clouds, and the CS^+ molecular ion is the first sulphur-bearing molecular detected in diffuse interstellar clouds.[6] Because CS^+ is a short-lived and highly reactive diatomic molecular ion, the CS^+ ion is usually considered as an important precursor and an intermediate in the formation of HCS^+.[7,11] The protonated molecular ion HCS^+[2] has been detected in the interstellar medium through radio-astronomical spectra, and has attracted extensive attention to understand the sulfur chemistry of interstellar clouds. In spectroscopy, precise and reliable spectroscopic constants and vibrational properties of molecules are effective in investigating properties of diatomic molecules. The molecular constants of CS^+ can be used as a diagnostic of the CS^+ abundancy in outer space.

On the theoretical side, a number of previous studies have aimed to understand the low-lying electronic states of CS^+ ion. In 1985, Larsson[8] used the complete active space self-consistent field (CASSCF) and configuration interaction methods to calculate potential energy curves (PECs) and spectroscopic constants for the $X^2\Sigma^+$, $A^2\Pi$, and $B^2\Sigma^+$ states of CS^+. Based on the CASSCF wave functions, he also obtained the electronic transition moments for the $A^2\Pi$–$X^2\Sigma^+$, $B^2\Sigma^+$–$X^2\Sigma^+$, and $B^2\Sigma^+$–$A^2\Pi$ transitions, and evaluated the radiative lifetimes of the $A^2\Pi$ and $B^2\Sigma^+$ states. In 2008, Honjou[9] studied the potential energies of the $X^2\Sigma^+$, $A^2\Pi$, $B^2\Sigma^+$, and $C^2\Sigma^+$ states of CS^+ by employing the *ab initio* method and simulated the photoelectron spectrum of CS. In 2010, Chenel *et al.*[10] studied the adiabatic potentials and couplings of the $^{2,4}\Sigma$ and $^{2,4}\Pi$ states in the CS^+ system employing the multireference configuration interaction (MRCI) method and obtained the charge transfer cross sections using the quantum and semiclassical approaches. Later, the vibrational levels for $X^2\Sigma^+$ and $A^2\Pi$ states of CS^+ were determined by Wang *et al.*[7] and Kaur *et al.*[11] at MRCI level of theory. In 2013, Li *et al.*[12] used the MRCI method with Davison size-extensivity correction (+Q) to calculate the potential energy curves of the low-lying 18 Λ–S electronic states of CS^+ correlating with the two lowest dissociation limits.

On the experimental side, Coxon[13] measured the intensity and wavelength for the CS^+ ($A^2\Pi$–$X^2\Sigma^+$) band system excited by the reaction of metastable He with CS_2. Latter, Tsuji *et al.*[14] and Cossart *et al.*[15] measured and analyzed

*Project supported by the National Key Research and Development Program of China (Grant Nos. 2017YFA0402300 and 2017YFA0403200), the National Natural Science Foundation of China (Grant Nos. 11474032, 11534011, U15302611, and 1404180), and China Postdoctoral Science Foundation (Grant No. 2018M631404).

†These authors contributed equally to this work.
‡Corresponding author. E-mail: lirei01@163.com
§Corresponding author. E-mail: wu_yong@iapcm.ac.cn

© 2019 Chinese Physical Society and IOP Publishing Ltd

the CS^+ ($B^2\Sigma^+$–$X^2\Sigma^+$) emission spectrum in the 220–340 nm region. In 2002, Liu *et al.*[16] studied the absorption spectrum of the (5,0) and (6,0) bands of the $X^2\Sigma^+ \rightarrow A^2\Pi$ transition of CS^+ employing velocity modulation absorption spectroscopy. Recently, Li *et al.*[17] measured the absorption spectrum of the (2,1) band in the $A^2\Pi$–$X^2\Sigma^+$ system of CS^+ by using the optical heterodyne velocity modulation absorption spectroscopy.

Although CS^+ ion has great significance in astrophysical environments, the accurate and systematic study of the absorbed cross sections is limited and scarce. The previous studies of CS^+ are mainly limited on the basic spectroscopic constants and molecular structure calculations. In the present work, the PECs and transition dipole moments (TDMs) are computed by employing the *ab initio* method. Based on the calculated molecular structure data, the vibrational energy levels, vibrational wave functions, and spectroscopic parameters of bound states of CS^+ are obtained by solving the nuclear Schrödinger equations. Finally, the rovibrational transition lines of the considered states of CS^+ are calculated for different temperatures and pressure conditions.

This article is organized as follows. In Section 2, we briefly outline the computational methods for the calculations of PECs, TDMs, vibrational energy levels, and opacity. In Section 3, we discuss our results for the spectroscopic properties of the $X^2\Sigma^+$, $A^2\Pi$, and $X^2\Sigma^+$ states, the corresponding vibrational energy levels, TDMs, and opacity. Finally, a brief summary is given in Section 4.

2. Theoretical method

In this work, electronic states of CS^+ are calculated with Molpro 2010[21] suite of quantum chemical procedure. The point group of CS^+ is $C_{\infty v}$, and all the calculations are done in the C_{2v} subgroup. The electronic states of CS^+ are described by irreducible representations of C_{2v}, and the corresponding relationship between the electronic states and irreducible representations of C_{2v} are $\Sigma^+ = A_1$, $\Sigma^- = A_2$, $\Pi = B_1+B_2$, and $\Delta = A_1+A_2$. For the basis sets adopted in the calculations, the contracted Gaussian-type basis sets aug-cc-pwCV5Z-DK[22–24] are chosen for C and S atoms, respectively. To obtain the precise PECs of the low-lying states of CS^+, single point energies at a series of internuclear distances are computed. The calculated process of single point energy includes the following three steps. First, the molecular orbitals (MOs) of $X^2\Sigma^+$ are computed with the Hartree–Fock (HF) self-consistent field method. Then, the 3 lowest Λ–S states of CS^+ are calculated by the state-averaged complete active space self-consistent field (SA-CASSCF)[25,26] using HF MOs as the starting orbitals. Finally, utilizing the reference wave functions obtained from the SA-CASSCF calculation, the internally contracted MRCI method is adopted to compute the single point energy of the electronic state. In the above SA-CASSCF calculation, the selection of active space is very important for the precision of single point energy. Hence, different active spaces have been tested, and finally eight outermost MOs (four A_1, two B_1, and two B_2) are selected as the active space, corresponding to 2s2p (C) and 3s3p (S) atomic orbitals. In the MRCI calculation, a total of 10 electrons ($2s^22p^2$ electrons of C and $3s^23p^4$ electrons of S) of CS^+ are taken into account in the computation of electronic correlation energy. The Davison size-extensivity correction[27–29] (+Q) is also included in the MRCI calculation to balance the the size-consistency error. The scalar relativistic effect is computed with third-order Douglas-Kroll[30] and Hess[31] integrals.

Under the Born–Oppenheimer approximation, the electronic Schrödinger equation of diatomic molecules can be written as

$$\hat{H}_e \Psi_e(r,R) = E_e(R)\Psi_e(r,R), \tag{1}$$

in which $\Psi_e(r,R)$ and $E_e(R)$ are the eigen-function and eigen-energy, respectively. $\hat{H}_e$ is the Hamiltonian for the N electrons diatomic molecules given by

$$\hat{H}_e = \sum_{i=1}^{N}\left(-\frac{1}{2}\nabla_i^2\right) + \sum_{i=1}^{N}\left(-\frac{Z_a}{r_{ai}} - \frac{Z_b}{r_{bi}}\right) + \sum_{i<j=1}^{N}\left(\frac{1}{r_{ij}}\right) + \frac{Z_a Z_b}{R}, \tag{2}$$

where Z_a and Z_b are the charge numbers of nuclei A and B.

On the basis of calculated energies of electronic states, the eigenvalues and wave functions of vibration-rotation states can be obtained by solving the following radical nuclear Schrödinger equation utilizing LEVEL program:[32]

$$\left[-\frac{1}{2\mu}\frac{d^2}{dR^2} + E_e(R)\right]\chi_{vJ}(R) = E_{vJ}\chi_{vJ}(R), \tag{3}$$

where $E_{vJ}(R)$ is the vibration-rotation level.

The Einstein coefficient between two vibration-rotation levels is defined as

$$A_{v'j',v''j''} = \frac{4}{3}\alpha^3\omega^3_{v'j',v''j''}\frac{S_{J'J''}}{2J''+1}, \tag{4}$$

where α is the fine-structure constant, $\omega_{v'j',v''j''}$ is the transition frequency of two vibration-rotation levels, and line strength ($S_{J'J''}$) and Hönl–London factor[33] ($\varphi_{J',J''}$) are determined by

$$S_{J'J''} = |\langle\chi_{v'J'}|D(R)|\chi_{v''J''}\rangle|^2\varphi_{J'J''}, \tag{5}$$

$$\varphi_{J',J''} = \begin{cases} J''-1, & \text{P}-\text{branch}, \\ J'', & \text{Q}-\text{branch}, \\ J''+1, & \text{R}-\text{branch}. \end{cases} \tag{6}$$

Total internal partition function $Q(T)$ is summed over the concerned electronic state weighed by the Boltzmann factor utilizing

$$Q = \sum_{i=1}^{n} Q_{ei}Q_{vi}Q_{ri}\exp\left(-\frac{T_i hc}{kT}\right), \tag{7}$$

in which T_i is the excitation energy of electronic state i, and T is the environment temperature. $Q_{ei} = (2S+1)(2-\delta_{\Lambda,0})$, where S is the electronic spin quantum number, $2S+1$ is the multiplicity, Λ is the electronic orbital quantum number: 0, 1, 2, 3, ... for Σ, Π, Δ, Φ, ... electronic states, respectively, and δ is the Kronecker delta. $Q_{vi} \times Q_{ri}$ is the summation over all possible rovibrational de-excitation transitions within the electronic state i, and $Q_{vi} \times Q_{ri} = (2J''+1)\sum_{v''J''} e^{-\Delta E_{v''J'',00}/kT}$,where $\Delta E_{v''J'',00}$ is the excitation energy of state (i, v'', J'') and 0 for the ground state.

The integrated line strength is the molecular opacity,[34–36] which is given by

$$S = \frac{A(2J'+1)\exp(-E''hc/kT)[1-\exp(-\Delta E_{v'J',00}/kT)]}{8\pi(\Delta E_{v'J',00}/hc)^2 Q}, \tag{8}$$

where E'' is the excitation energy of the lower electronic state in units of cm^{-1}, $\Delta E_{v'J',00}$ is rovibrational excitation energy of energy level v', J', $Q(T)$ is the total internal partition function, and the Einstein A-values for each line are computed using formula (4).

3. Results and discussion

3.1. Potential energy curves, spectroscopic constants, and vibrational levels

As plotted in Fig. 1, three electron states, namely, $X^2\Sigma^+$, $A^2\Pi$, and $B^2\Sigma^+$, are computed. All of the states that are correlated to the two lowest dissociation limits $C(^3P) + S^+(^4S)$ and $C^+(^2P) + S(^3P)$ of CS^+ are typically bound and calculated with the MRCI+Q method utilizing the aug-cc-pwCV5Z-DK basis set.

On the basis of the calculated PECs, the spectroscopic constants are obtained with the numerical method and listed in Table 1, including adiabatic transition energies T_e, harmonic vibrational frequencies ω_e, anharmonic terms $\omega_e\chi_e$, rotational constants B_e, and equilibrium distances R_e. To verify the accuracy of our calculation, Table 1 also gives the available theoretical results and experimental values. For the ground state $X^2\Sigma^+$, the B_e and R_e are in good agreement with the experimental results, and the deviations are 0.002046 cm^{-1} and

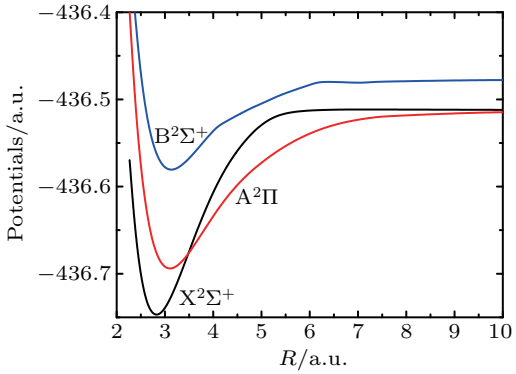


Fig. 1. Calculated potential energy curves for the $X^2\Sigma^+$, $A^2\Pi$, and $B^2\Sigma^+$ states of CS^+.

Table 1. Computed and experimental spectroscopic constants of CS^+.

State		T_e/cm^{-1}	ω_e/cm^{-1}	$\omega_e\chi_e$/cm^{-1}	B_e/cm^{-1}	R_e/Å
$X^2\Sigma^+$	this work	0.0	1366.15	7.0507	0.8657	1.4946
	Expt.[a]	0.0	1377.49(16)	7.812(39)	0.867746(91)	1.492156(78)
	Expt.[b]	0.0	1384(30)			
	Calc.[d]	0.0	1358.45	7.64	0.8575	1.501
	Calc.[e]	0.0	1369			1.503
	Calc.[f]	0.0	1357	7.6		1.503
	Calc.[g]	0.0	1371.6075	7.7925	0.8609	1.4981
	Calc.[i]		1375.02	7.6416	0.8628	1.4964
$A^2\Pi$	this work	11709	1016.11	6.5751	0.7178	1.6406
	Expt.[a]	11987.25(67)	1013.90(37)	6.842(48)	0.718739(90)	1.63955(10)
	Expt.[b]		972(30)			
	Expt.[c]				0.7029211(14)	
	Calc.[d]	11875.8	988.34	6.41	0.7074	1.653
	Calc.[e]	11940	1004			1.650
	Calc.[f]	12079	1001	7.8		1.650
	Calc.[g]	11675.8809	1014.2091	6.5497	0.7143	1.6445
	Calc.[i]		1010.42	6.5571	0.7144	1.6442
$B^2\Sigma^+$	this work	36869	929.18	8.6552	0.7050	1.6555
	Expt.[b]		868(30)			
	Expt.[h]	36509	911(3)	6.5(1)		1.665
	Calc.[d]	36993.5	920.6	6.44	0.6953	1.667
	Calc.[e]	35980	907			1.670
	Calc.[f]	35865	895	7.5		1.671
	Calc.[g]	36131.7388	912.1725	7.6352	0.6984	1.6642

Note: For the experimental values, the inaccuracy of measurement is depicted in the bracket.

[a]Ref. [16], [b]Ref. [18], [c]Ref. [17], [d]Ref. [8], [e]Ref. [19], [f]Ref. [9], [g]Ref. [12], [h]Ref. [14], [i]Ref. [7].

Table 2. Calculated vibrational levels E_v for the $X^2\Sigma^+$ states of CS^+ (in cm^{-1}).

v	This work	Calc.[a]	Calc.[b]	Calc.[c]	Expt.[d]
0	682.03	677	685.61	681.3	686.84
1	2030.93	2018	2045.38	2032.8	2048.70
2	3363.61	3344	3389.79	3369.1	3394.90
3	4689.26	4655	4718.79	4690.0	4725.41
4	6003.10		6032.37	5995.6	6040.23
5	7302.46		7330.49	7285.9	7339.32
6	8586.55		8613.11	8560.8	8622.66
7	9855.21		9880.25	9820.3	9890.24
8	11108.36		11131.81	11064.4	11142.03
9	12346.01		12367.81	12293.0	12378.00
10	13567.99		13588.19	13506.1	13598.14
11	14774.28		14792.93	14703.7	14802.42
12	15965.45		15981.98	15885.7	15990.82
13	17142.56		17155.31	17052.2	17163.32
14	18306.03		18312.86	18202.9	18319.90
15	19454.78		19454.60	19337.9	19460.53
16	20587.03		20580.48	20457.2	20585.20
17	21701.76		21690.45	21560.5	21693.87
18	22799.43		22784.44	22648.0	22786.53
19	23881.06		23862.42	23719.6	23863.16

[a]Ref. [9], [b]Ref. [7], [c]Ref. [11], [d]Ref. [16].

Table 3. Calculated vibrational levels E_v for the $A^2\Pi$ states of CS^+ (in cm^{-1}).

v	This work	Calc.[a]	Calc.[b]	Calc.[c]	Expt.[d]
0	12492.54	12485.25	12491.05	12466.3	12492.533
1	13494.24	13469.25	13488.51	13456.8	13492.749
2	14482.80	14440.25	14472.57	14434.0	14479.281
3	15458.15	15397.25	15443.18	15397.8	15452.129
4	16421.16	16339.25	16400.31	16348.2	16411.293
5	17373.84	17267.25	17343.92	17285.0	17356.773
6	18314.97	18183.25	18273.96	18208.3	18288.569
7	19240.73	19085.25	19190.38	19117.9	19206.681
8	20150.60	19975.25	20093.09	20013.9	20111.109
9	21047.01		20982.04	20896.1	21001.853
10	21930.37		21857.15	21764.4	21878.913
11	22799.63		22718.31	22618.8	22742.289
12	23654.62		23565.43	23459.0	
13	24495.41		24398.41	24285.1	
14	25321.87		25217.12	25096.8	
15	26133.83		26021.46	25893.9	
16	26931.14		26811.28	26676.5	
17	27713.71		27586.46	27444.2	
18	28481.41		28346.88	28197.1	
19	29234.14		29092.39	28934.9	

[a]Ref. [9], [b]Ref. [7], [c]Ref. [11], [d]Ref. [16].

and 0.002444 Å, respectively. For the low lying excited state $A^2\Pi$, the calculated transition energy T_e is 11709 cm^{-1}, while the recent experimental result is 11987.25 cm^{-1}, the deviation is only 278.25 cm^{-1}. Equilibrium distance R_e value is in accord with the results of experiment, with the error of 0.00105 Å. For the second excited state $B^2\Sigma^+$, the adiabatic excitation energy is 36869 cm^{-1}, as shown in Table 1. Moreover, the vertical excitation energy of $B^2\Sigma^+$ is 40271 cm^{-1} and the energy gap between $B^2\Sigma^+$ and $A^2\Sigma^+$ is 8122 cm^{-1} at the asymptotic region. The harmonic vibrational frequencies ω_e and anharmonic terms $\omega_e\chi_e$, which are determined by the vibrational terms, are suitably consistent with the experimental results, within the maximum differences of 18.18 cm^{-1} and 2.1552 cm^{-1}, respectively. The differences of T_e and R_e are 0.9% and 0.6% between our results and experimental values, respectively.

To confirm the accuracy of our calculation, the vibrational levels of the $X^2\Sigma^+$, $A^2\Pi$, and $B^2\Sigma^+$ states are also given. In Tables 2–4, our calculated results are close to both of the experimental results and the existing theoretical values. For the ground state $X^2\Sigma^+$, our computed vibrational levels are up to $v = 19$, the results are in accord with the measurement results.[16] For the $A^2\Pi$ state, the maximum deviation is 2.225% in comparing with the experimental data.[16] In addition, our calculated energy level of the $B^2\Sigma^+$ state is close to the previously available theoretical result.[9] All the spectroscopy constants and vibrational levels can provide important parameters for the calculation of the spectrum.

Table 4. Calculated vibrational levels E_v for the $B^2\Sigma^+$ states of CS^+ (in cm^{-1}).

v	This work	Calc.[a]
0	37331.82	36956
1	38244.30	37837
2	39137.29	38701
3	40008.82	39548
4	40864.52	40378
5	41708.09	41190
6	42535.10	41984
7	43345.11	42760
8	44138.99	43517
9	44914.84	44255
10	45671.53	
11	46409.47	
12	47128.06	
13	47820.10	
14	48466.36	
15	49053.60	
16	49604.63	
17	50134.63	
18	50643.26	
19	51134.21	

[a]Ref. [9].

3.2. Electronic transition dipole moments and radiative lifetimes

The dipole moment (DM) and TDMs of the low-lying states are calculated by utilizing MRCI methods. The DM and TDM curves are presented in Fig. 2. As shown in Fig. 2, the DM for the $X^2\Sigma^+$ state changes with the increasing bond, and the calculated DM of the state tends to be a negative value because of the dissociation limits $C(^3P) + S^+(^4S)$ of the CS^+ ion. The TDMs from the $X^2\Sigma^+$ state to the excited states $A^2\Pi$ and $B^2\Sigma^+$ are calculated as a function of the internuclear distance, also depicted in Fig. 2. The TDM of $X^2\Sigma^+$–$B^2\Sigma^+$ is much larger than that of $X^2\Sigma^+$–$A^2\Pi$ as displayed in Fig. 2.

The maximum TDM of $X^2\Sigma^+$–$B^2\Sigma^+$ is located at the distance of $R = 5.48$ a.u.

The Frank–Condon factors of the $X^2\Sigma^+$–$A^2\Pi$ and $X^2\Sigma^+$–$B^2\Sigma^+$ systems, which are calculated with the aid of the LEVEL program, are listed in Table 5. The computed values, whose change trends are irregular, are in good agreement with the previous experimental results. As shown in Table 5, the Frank–Condon factor of the 0–0 band is 0.0265 for $X^2\Sigma^+$–$A^2\Pi$, which is close to the experimental value of 0.0355. While the Frank–Condon factors for the $X^2\Sigma^+$–$B^2\Sigma^+$ system are also obtained for the first time.

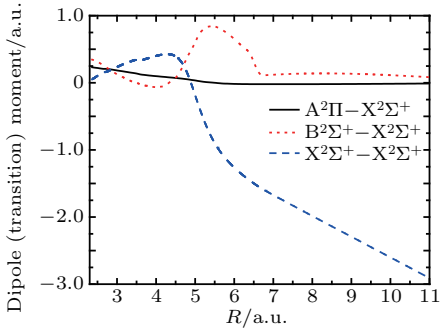


Fig. 2. Transition dipole moments for different states of CS^+ as a function of internuclear distance R.

Table 5. Franck–Condon factors for the $A^2\Pi$ –$X^2\Sigma^+$ and $B^2\Sigma^+$–$X^2\Sigma^+$ transitions of CS^+.

Transition	v''/v'		0	1	2	3	4	5	6
$A^2\Pi$–$X^2\Sigma^+$	0	this work	0.0265	0.0828	0.1396	0.1690	0.1652	0.1386	0.1031
		Expt.[a]	0.0355	0.1019	0.1591	0.1795	0.1641	0.1294	0.0913
		Expt.[b]	0.0358	0.1030	0.1611	0.1809	0.1645	0.1291	0.0906
	1	this work	0.1067	0.1774	0.1287	0.0408	0.0005	0.0180	0.0579
		Expt.[a]	0.1345	0.1906	0.1114	0.0216	0.0018	0.0359	0.0772
		Expt.[b]	0.1343	0.1906	0.1110	0.0207	0.0023	0.0379	0.0797
	2	this work	0.2055	0.1238	0.0044	0.0342	0.0891	0.0754	0.0266
		Expt.[a]	0.2353	0.0977	0.0002	0.0612	0.0973	0.0573	0.0098
		Expt.[b]	0.2336	0.0974	0.0002	0.0622	0.0978	0.0564	0.0089
	3	this work	0.2462	0.0116	0.0619	0.0962	0.0214	0.0054	0.0504
		Expt.[a]	0.2525	0.0006	0.0941	0.0811	0.0042	0.0233	0.0681
		Expt.[b]	0.2508	0.0007	0.0937	0.0812	0.0041	0.0241	0.0694
	4	this work	0.2042	0.0313	0.1140	0.0066	0.0387	0.0758	0.0269
		Expt.[a]	0.1860	0.0682	0.0984	0.0003	0.0676	0.0651	0.0074
	5	this work	0.1245	0.1388	0.0276	0.0503	0.0735	0.0021	0.0327
		Expt.[a]	0.0997	0.1756	0.0051	0.0846	0.0489	0.0030	0.0570
	6	this work	0.0579	0.1842	0.0134	0.0978	0.0003	0.0595	0.0479
		Expt.[a]	0.0403	0.1823	0.0485	0.0774	0.0087	0.0777	0.0222
$B^2\Sigma^+$–$X^2\Sigma^+$	0	this work	0.1304	0.2511	0.2546	0.1815	0.1029	0.0488	0.0200
	1	this work	0.2619	0.1377	0.0019	0.0544	0.1417	0.1582	0.1184
	2	this work	0.2722	0.0008	0.1090	0.1049	0.0103	0.0212	0.0934
	3	this work	0.1874	0.0783	0.1031	0.0012	0.0859	0.0818	0.0100
	4	this work	0.0948	0.1815	0.0025	0.0982	0.0456	0.0085	0.0779
	5	this work	0.0374	0.1748	0.0558	0.0719	0.0160	0.0873	0.0152
	6	this work	0.0119	0.1065	0.1511	0.0001	0.0974	0.0085	0.0470

[a]Ref. [16], [b]Ref. [13].

On basis of this transitions information, the radiative lifetimes of the corresponding vibrational levels are obtained. The radiative lifetimes are determined by the summation of the Einstein coefficients $A_{v'v''}$

$$\tau = \left(\sum_{v'} A_{v'v''}\right)^{-1}. \tag{9}$$

The Einstein coefficient, which is a parameter for spontaneous emission between vibrational levels v' and v'', is defined as

$$A_{v'v''} = 2.026 \times 10^{-6} \Delta E^3_{v'v''} (\mathrm{TDM})^2 \left(\int \psi_{v'} \psi_{v''} \mathrm{d}r\right)^2, \tag{10}$$

where $\Delta E_{v'v''}$ is the energy gap of the vibrational levels v' and v'' in units of cm^{-1}, TDM is the average transition dipole moment in the atomic unit, while the last term $(\int \psi_{v'} \psi_{v''} \mathrm{d}r)^2$ is the Frank–Condon factors for the vibrational levels v' and v'', and the radiative lifetime is in units of second.

The concrete calculation results for the selected vibrational levels for transitions of $A^2\Pi$ and $B^2\Sigma^+$ are tabulated in Table 6. The longest radiative lifetime of $A^2\Pi$ is 32.90 μs owing to the small transition dipole moments of the $X^2\Sigma^+$–$A^2\Pi$ transition.

Table 6. Radiative lifetimes of several electronic states at low-lying vibrational levels of CS^+ (in μs).

Electronic state		Radiative lifetimes of upper vibrational levels				
		$v' = 0$	$v' = 1$	$v' = 2$	$v' = 3$	$v' = 4$
$A^2\Pi$	this work	32.90	27.07	23.23	20.51	18.47
	Calc.[a]	27.7	22.1	18.6	16.2	14.4
	Calc.[b]	22.3	17.1	14.0	12.0	10.5
$B^2\Sigma^+$	this work	1.96	2.01	2.07	2.13	2.19
	Calc.[a]		1.99	1.69	1.47	1.32
	Calc.[b]	2.49				

[a]Ref. [20], [b]Ref. [8].

3.3. Opacity

The partition function and opacity of CS^+ are computed on the basis of the results of vibrational level, wavefunction, DM, and TDM. For the partition function, which is an important parameter in radiative transfer and spectroscopy analysis in the astrophysical field, is calculated with different temperatures in the range of 10–4500 K. In this work, the values of the partition function are obtained by summing all over the ro-vibrational states of the lowest three states, and the results of the partition function are listed in Table 7, and the corresponding figure is rendered in Fig. 3. As shown in the results, the partition functions augment with increase of the temperature according to formula (7).

In our calculation, the opacity is convolved by a Lorentzian line profile with width corresponding to collisional broadening.[36–38] By utilizing a canonical collisional broadening cross section of 10^{-16} cm^2 with a line width proportional to the pressure, figure 4 presents the opacities of CS^+ at the temperatures of 300 K, 500 K, 1000 K, and 4500 K with the pressure of 100 atms. As shown in Figs. 4(a)–4(d), the spectra are mainly lying in the range of ultraviolet to far-infrared, which include three bands obtaining from the transitions of the three electron states, namely, $X^2\Sigma^+$–$X^2\Sigma^+$, $X^2\Sigma^+$–$A^2\Pi$, and $X^2\Sigma^+$–$B^2\Sigma^+$, from right to left. From Figs. 4(a) and 4(b), it is clearly observed that each band system is different at temperatures of 300 K and 500 K. As depicted in Figs. 4(a) and 4(b), the band systems corresponding to $X^2\Sigma^+$–$A^2\Pi$ and $X^2\Sigma^+$–$B^2\Sigma^+$ appear at 243 nm and 683 nm, respectively, which are associated with the short-wave ultraviolet range. For the band of $X^2\Sigma^+$–$X^2\Sigma^+$, the strong pure rotational lines are located in the range of $\lambda > 10$ μm. And the vibrational band of $\Delta v = 1$ appears near 7.3 μm. It can be found that the opacities of molecular are distinguishable and weak in the range of 1200–3600 nm. Meanwhile, as temperature increases, the cross section grows and the systems of different bands are fuzzy, which contribute to the enhanced population of the vibrational excited and electronic states with the high temperature. At the same time, the pure rotational spectra are reduced because of the decreased populations of the ground state as the temperature increases.

Table 7. Partition function Q for CS^+ as a function of temperature.

T/K	Q
10	8.41
100	81.01
300	242.85
500	412.65
1000	946.04
2000	2634.11
4500	11253.22

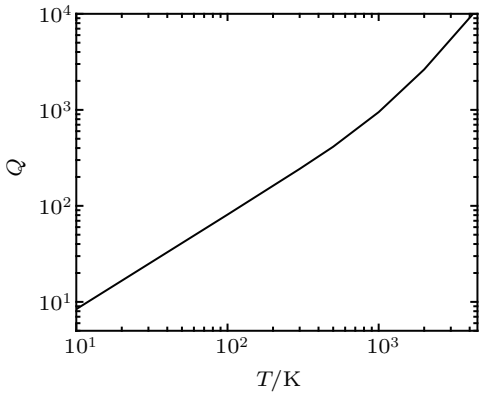


Fig. 3. Partition function for CS^+.

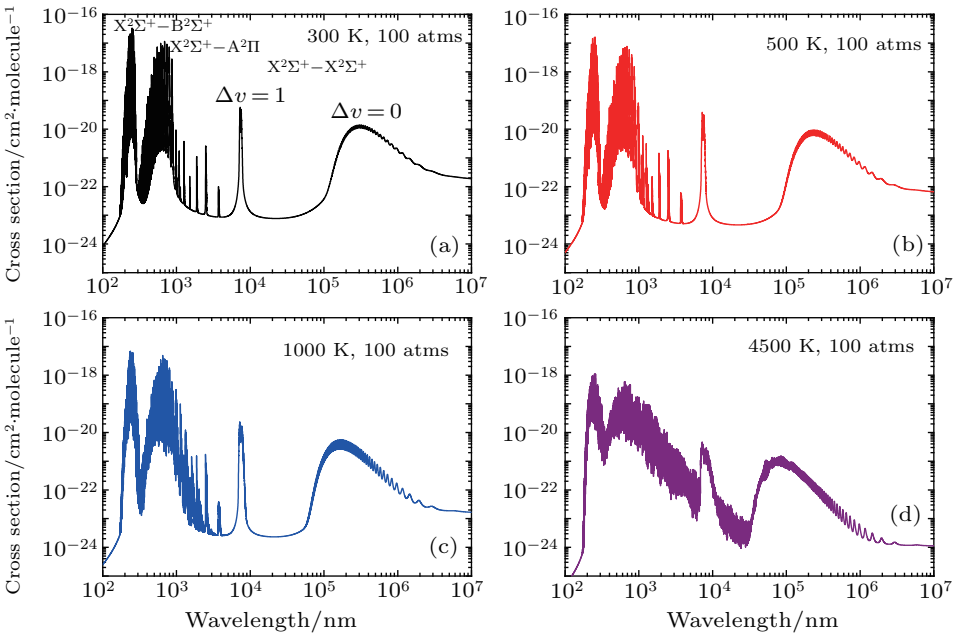


Fig. 4. Opacities of CS^+ ro-vibrational transitions for temperatures of (a) 300 K, (b) 500 K, (c) 1000 K, (d) 4500 K and a pressure of 100 atms. Note that three electronic states of $X^2\Sigma^+$, $A^2\Pi$, and $B^2\Sigma^+$ have been included in the present calculations.

4. Conclusion

In the present work, the PECs of the $X^2\Sigma^+$ state and two excited states $A^2\Pi$ and $X^2\Sigma^+$ are calculated with the MRCI+Q method. On the basis of the PECs, the corresponding spectroscopic constants and vibrational levels are obtained, which agree well with the experimental results. The TDMs of the two excited states to the ground state $X^2\Sigma^+$ are obtained, and the radiative lifetimes of $A^2\Pi$ and $X^2\Sigma^+$ states are also obtained. The cross sections for the three lowest lying states are given at 300 K, 500 K, 1000 K, and 4500 K under the pressure of 100 atms. It is shown that the spectra are clearly separated for the temperatures of 300 K and 500 K both for the vibrational transition and the electron transitions. However, with the increase of the temperature, the population on the excited states cannot be ignored, and the boundaries of the lines become blurred. At the same time, the partition functions are also found in the range of 10–4500 K. The accuracy of electronic structures and opacities of molecule for the low-lying three states provide more information to model the atmosphere calculation.

References

[1] Penzias A A, Solomon P M, Wilson R W and Jefferts K H 1971 *Astrophys. J. Lett. Ed.* **168** L53
[2] Thaddeus P, Guelin M and Linke R A 1981 *Astrophys. J. Lett. Ed.* **246** L41
[3] Saito S, Kawaguchi K, Yamamoto S, Ohishi M, Suzuki H and Kaifu N 1987 *Astrophys. J. Lett. Ed.* **317** L115
[4] Yamamoto S, Saito S, Kawaguchi K, Kaifu N, Suzuki H and Ohishi M 1987 *Astrophys. J. Lett. Ed.* **317** L119
[5] Bell M B, Avery L W and Feldman P A 1993 *Astrophys. J. Lett.* **417** L37
[6] Ferlet R, Roueff E, Czarny J and Felenbok P 1986 *Astron. Astrophys.* **168** 259
[7] Wang L, Yang C L, Wang M S, Ma X G and Liu W W 2011 *Comput. Theor. Chem.* **976** 94
[8] Larsson M 1985 *Chem. Phys. Lett.* **117** 331
[9] Honjou N 2008 *Chem. Phys.* **344** 128
[10] Chenel A, Mangaud E, Justum Y, Talbi D, Bacchus-Montabonel M C and Desouter-Lecomte M 2010 *J. Phys. B: At. Mol. Opt. Phys.* **43** 245701
[11] Kaur R and Dhilip Kumar T J 2016 *Chem. Phys.* **479** 36
[12] Li R, Wei C L, Sun Q X, Sun E P, Jin M X, Xu H F and Yan B 2013 *Chin. Phys. B* **22** 123103
[13] Coxon J A, Marcoux P J and Setser D W 1976 *Chem. Phys.* **17** 403
[14] Tsuji M, Obase H and Nishimura Y 1980 *J. Chem. Phys.* **73** 2575
[15] Cossart D, Horani M and Vervloet M 1993 *Am. Inst. Phys. Conf. Proc.* 312367
[16] Liu Y Y, Duan C X, Liu J J, Wu L, Xu C X, Chen Y Q, Hamiltion P A and Davies P B 2002 *J. Chem. Phys.* **116** 9768
[17] Li C L, Deng L H, Zhang Y, Yang X H and Chen Y Q 2010 *J. Mol. Spectrosc.* **264** 75
[18] Frost D C, Lee S T and McDowell C A 1972 *Chem. Phys. Lett.* **17** 153
[19] Honjou N 2006 *Chem. Phys.* **324** 413
[20] Blöcker J H, Reinsch E A, Rosmus P, Werner H J and Knowles P J 1990 *Chem. Phys.* **147** 99
[21] Werner H J, Knowles P J, Knizia G, *et al.* 2010 *MOLPRO: a Package of ab initio Programs*
[22] Kendall R A, Dunning T H and Harrison R J 1992 *J. Chem. Phys.* **96** 6796
[23] Peterson K A and Dunning T H 2002 *J. Chem. Phys.* **117** 10548
[24] Woon D E and Dunning T H 1993 *J. Chem. Phys.* **98** 1358
[25] Knowles P J and Werner H J 1985 *Chem. Phys. Lett.* **115** 259
[26] Werner H and Knowles P J 1985 *J. Chem. Phys.* **82** 5053
[27] Langhoff S R and Davidson E R 1974 *Int. J. Quantum. Chem.* **8** 61
[28] Knowles P J and Werner H J 1988 *Chem. Phys. Lett.* **145** 514
[29] Werner H J and Knowles P J 1988 *J. Chem. Phys.* **89** 5803
[30] Douglas M and Kroll N M 1974 *Ann. Phys.* **82** 89
[31] Hess B A 1986 *Phys. Rev. A.* **33** 3742
[32] Le Roy R J 2002 *LEVEL 7.5: a Computer Program for Solving the Radial Schrödinger Equation for Bound and Quasibound Levels* (University of Waterloo, Chemical Physics Research Report CP-655)
[33] Herzberg G 1950 *Molecular Spectra and Molecular Structure, Spectra of Diatomic Molecules* (New York: Van Nostrand Reinhold)
[34] Dulick M, Bauschlicher C W, Burrows A, Sharp C M, Ram R S and Bernath P 2003 *Astrophys. J.* **594** 651
[35] Xu X S, Dai A Q, Peng Y G, Wu Y and Wang J G 2018 *J. Quant Spectrosc. Radiat Transf* **206** 172
[36] Shi Y B, Stancil P C and Wang J G 2013 *A&A* **551** A140
[37] Meng G W, Wang J G, Wang X R, Li J H and Zhang W Y 2016 *MRE* **1** 5
[38] Bernath P F 1995 *Spectra of Atoms and Molecules* (Oxford: Oxford University Press)